

Artefact subspace reconstruction for both EEG and fNIRS co-registered signals

N Aloui, A Planat-Chrétien, S Bonnet

Abstract—Combining electroencephalography (EEG) to functional near-infrared spectroscopy (fNIRS) is a promising technique that has gained momentum thanks to their complementarity. While EEG measures the electrical activity of the brain, fNIRS records the variations in cerebral blood flow and related hemoglobin concentrations. However, both modalities are typically contaminated with artefacts. Muscle and eye artefacts, affect the EEG signals, while hemodynamic and oxygenation changes in the extracerebral compartment due to systemic changes (superficial layer) corrupt the fNIRS signals. Moreover, both signals are sensitive to sensor motion artefacts characterized by large amplitude. There are several well-established methods for removing artefacts for both modalities. The objective of this paper is to apply a common approach to denoise both EEG and fNIRS signals. Indeed Artifact Subspace Reconstruction (ASR) method, which is an automatic, online-capable and efficient method for deleting transient or large-amplitude EEG artefacts, can be a good alternative to also denoise fNIRS signals. In this paper, we first propose, a new more comprehensive formulation of ASR. Then, we study the effectiveness of the method in denoising both the EEG and fNIRS signals.

Clinical Relevance—Denoising EEG and fNIRS signals with the same method would facilitate the combination of both modalities and hence, help in improving the robustness of neural-based diagnostics such as the Alzheimer’s disease.

I. INTRODUCTION

It is well known that EEG recordings are contaminated by many sources that are either **endogenous** (caused by cardiac, muscle as well as ocular activities) or **exogenous** (caused by power line noise, electrode movement, impedance mismatch). To handle these contaminants, different EEG artefact removal methods have been proposed such as statistical thresholding methods, blind source separation (BSS) and principal component analysis (PCA). Statistical thresholding methods such as those based on the signal variance discard signal portions whose variance exceeds a certain value. A calibration phase is then required to determine this threshold for each subject/session. The BSS-based approaches [1-2] separate data into cerebral and non-cerebral activities. To identify artifactual components, the method needs either a classifier or signals from auxiliary channels like electrooculography (EOG) signals.

N. Aloui (corresponding author) belongs to Commissariat à l’énergie atomique et aux énergies alternatives (CEA), 17 Avenue des Martyrs, 38000 Grenoble; e-mail: nadia.aloui@cea.fr.

Regarding PCA-based methods, their principle is as follows. The methods find orthogonal directions that maximize the variance in the observed data. Principal components (PCs) with large variance are usually discarded and the data is reconstructed from the remaining components. All these approaches delete noisy data which can cause an important loss of neural information.

Over the last years, we notice a remarkable use of ASR for denoising EEG signals [3-5]. ASR is an automatic PCA-based method that not only identifies the portions of data with artifacts but also denoise them. It is used in online applications to get rid of transient or large amplitude artifacts in EEG signals. An offline version of ASR is available in EEGLAB [6].

Similarly, fNIRS studies may be affected by physiological noise (endogenous sources) or motion artefacts (exogenous sources). Indeed, respiration and cardiac changes as well as systemic activities in the intra and extra cerebral compartments contribute to hemodynamics responses that may be confound with the targeted neurovascular coupling, leading to false positives or false negatives [7]. On the other hand, fNIRS signals may be contaminated by head movements, causing transient or large-amplitude artifacts. Several techniques have been proposed in the literature to deal with these motion artefacts and a review has been proposed in [8]. The authors compare the performance of different methods on real functional data acquired during a cognitive task. They compare PCA, spline interpolation, Kalman filtering, wavelet filtering and correlation-based signal improvement; they conclude that wavelet filtering is a promising and powerful technique for the correction of motion artifacts in fNIRS data.

In this paper, we evaluate the effectiveness of ASR to denoise fNIRS signals and show promising results combining EEG and fNIRS modalities in an identical pre-processing scheme. Our main goal is to use one single, robust and automatic data-denoising method to denoise signals from two commercial systems EEG and fNIRS. We first propose a more comprehensive formulation of ASR (section II); then we show some results (section III) on fNIRS measurements only and on combined fNIRS-EEG measurements. We discuss the obtained results before a conclusion.

S. Bonnet belongs to Commissariat à l’énergie atomique et aux énergies alternatives (CEA), 17 Avenue des Martyrs, 38000 Grenoble; e-mail: stephane.bonnet@cea.fr

A. Planat-Chrétien, belongs to Commissariat à l’énergie atomique et aux énergies alternatives (CEA), 17 Avenue des Martyrs, 38000 Grenoble; e-mail: anne.planat-chretien@cea.fr.

II. MATERIALS AND METHODS

A. Dataset and data preprocessing for EEG and fNIRS signals

We acquired a specific dataset with both EEG and fNIRS signals to figure out the method and validate the use of ASR for both modalities.

EEG data were recorded through ENOBIO system (NeuroElectrics) with only one electrode placed at Fp2 according to the international 10-20 system. Two additional electrodes for referencing and for ground were placed at mastoids. The EEG signal, sampled at 500 Hz, was first down-sampled at 100 Hz and then filtered using band-pass filter [0.5-40] Hz in order to remove drift and high-frequency noise.

fNIRS data were recorded with the dual wavelength continuous NIRSport2 system (NIRx Medical Technologies). We used a headband of 8 sources and 7 detectors and replaced one source by the EEG electrode (see Fig.1). The fNIRS signal, sampled at 20.34 Hz was oversampled at 100 Hz – cubic interpolation. The short-term fluctuations are subtracted from the signal through the use of a moving average.

Both systems were synchronized by means of TTL event triggers. The experimental procedure was approved by the Institutional Review Board. The protocol comprised 3 sessions and was performed on one volunteer. During a session, the volunteer was asked to blink by wrinkling his forehead every time a visual stimulus appears on the screen. The stimulus is repeated 10 times every 2 seconds before a rest period. The protocol is conceived to induce EEG artefacts via eye blinking, and fNIRS artifacts via motion artifacts (motion of the headband with respect to the forehead). Some data are shown in Fig.2. As the artifacts last almost 0.4 s (Fig.2), this guides us to choose values of some parameters of the ASR method such as the window length for computing variance thresholds.

B. ASR

Artifact subspace reconstruction (ASR) is a method for (online) artefact rejection that has been first introduced in [4]. For each sliding EEG window, a principal component analysis (PCA) is performed and a mechanism allows to identify clean versus noisy PCs. Contrary to standard PCA where noisy PCs are discarded for signal reconstruction, the key idea of ASR is to treat noisy PCs as missing information and estimate them by imposing some covariance constraints. This fact is usually quite hidden in the algorithm description and thus we propose in this paper to reformulate ASR in a more comprehensive way that may open different variants. The ASR method comports three distinct steps.



Figure 1. Optical sources (red points)/detectors (blue points) and EEG electrode positions (black point).

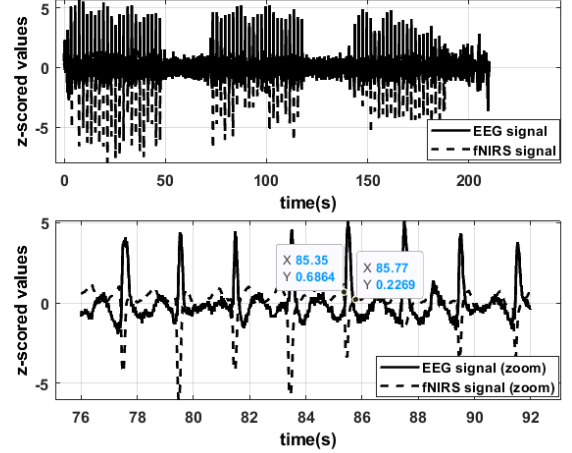


Figure 2. Visualization of raw data (z-scored). Top figure: data (one channel fNIRS, one channel EEG). Bottom figure: zoom.

In the first step (i.e. *calibration step*), the data is segmented into non-overlapping 1-second windows and each window delivers channelwise root-mean-square (RMS) value. The RMS time series is zscored and a window is said *clean* if the zscored RMS value for all channels are within a specified interval, typically $[-3.5, +5.5]$ in EEGLAB implementation. The clean data matrix \mathbf{X}_0 is formed by the concatenation of all the clean epochs. Hence, \mathbf{X}_0 depends implicitly on the chosen zscore interval.

The proportion of clean data is simply the ratio of the number of time samples within clean windows over the total number of time samples.

In the second step, the root-mean-square (RMS) threshold vector \mathbf{s}_0 is determined: the spatial covariance matrix \mathbf{C}_0 relative to \mathbf{X}_0 is first decomposed using eigenvalue decomposition (EVD) as $\mathbf{C}_0 = \mathbf{U}_0 \text{diag}(\boldsymbol{\lambda}_0) \mathbf{U}_0^T$ where $\mathbf{U}_0 = [\mathbf{u}_{0,1}, \dots, \mathbf{u}_{0,N_c}]$ and N_c is the number of channels. A PC score is computed as $\mathbf{y}_{0,i} = \mathbf{u}_{0,i}^T \mathbf{X}_0$. By looking at the RMS values of successive windows in $\mathbf{y}_{0,i}(t)$, one can deduce the mean/standard deviation of the RMS distribution $(\mu_{0,i}, \sigma_{0,i})$ and a RMS threshold is set as $s_{0,i} = \mu_{0,i} + \kappa \cdot \sigma_{0,i}$ where κ is an user-defined cutoff parameter. These values are collected in the $N_c \times 1$ vector \mathbf{s}_0 .

In the third step (i.e. *operating step*), PCA is performed on successive EEG epochs. Denote the current spatial covariance matrix by $\mathbf{C} = \mathbf{U} \text{diag}(\boldsymbol{\lambda}) \mathbf{U}^T$. Let $\mathbf{Y} = \mathbf{U}^T \mathbf{X}$ denote the $N_c \times N_t$ PC scores; where N_t is the number of time samples.

The variance λ_i of each score is compared to the threshold $\|\mathbf{u}_i^T \mathbf{U}_0 \cdot \text{diag}(\mathbf{s}_0)\|_2^2$ in order to decide if the principal component is clean or noisy.

Without loss of generality, let $\mathbf{Y}_A = \mathbf{U}_A^T \mathbf{X}$ denote the clean PC scores. The main idea of ASR is to compute the smallest-norm solution $\hat{\mathbf{Z}}$ to the unconstrained least-squares minimization problem

$$\phi(\mathbf{Z}) = \|\mathbf{U}_A^T \mathbf{C}_0^{1/2} \mathbf{Z} - \mathbf{Y}_A\|_F^2 \quad (1)$$

The matrix \mathbf{Z} can be interpreted as the ZCA-whitened EEG epoch where ZCA stands for zero-phase component analysis [9].

The denoised EEG epoch is finally given by

$$\mathbf{X}_{\text{denoised}} = \mathbf{C}_0^{1/2} \hat{\mathbf{Z}} = \mathbf{C}_0^{1/2} (\mathbf{U}_A^T \mathbf{C}_0^{1/2})^\dagger \mathbf{U}_A^T \mathbf{X} \quad (2)$$

It can be shown to be equivalent to the formulation in [4-5].

C. ASR applied to both EEG and fNIRS co-registered signals

Before computing artifact statistics, ASR applies to EEG data (both reference data \mathbf{X}_0 and \mathbf{X}) an IIR filter that is more sensitive to blinks (Delta: $f < 4$ Hz) and muscular activities (Gamma: $f > 30$ Hz) frequency content [3]. The filter is applied when computing the thresholds during the second step and the scores variances during the operating phase but it is not applied on the output signal. We expect that this filter, tailored to EEG artefacts, would not be useful to fNIRS signals (0.01-0.5 Hz). The effect of the ASR filter on fNIRS signals will be studied in the following section. Note that this filter is applied optionally which extends the scope of the ASR applications to connectivity analyses based on phase-related metrics.

III. RESULTS

To evaluate ASR, we report the percentage of clean portions on the denoised data $\mathbf{X}_{\text{denoised}}$ obtained through ASR process. To do so, we follow the same strategy that the one during the calibration phase of the ASR method but applied to the denoised data. The higher the percentage of clean portions, the more efficient has been the ASR process.

To do so, we compute the z-scores of the RMS values over the denoised data signal epochs and identify the clean portions as those in which the z-score values are within a certain interval.

We use this strategy to evaluate the effect of the filter in denoising the fNIRS signals. The percentage of the clean portions from the ASR denoised data with different cutoff parameters κ and different z-scores intervals is illustrated in Fig.3. As expected, the filter does not improve the artefacts correction, whatever the z-scores values, for almost all values of κ .

We further study the influence of the cutoff parameter involved in the ASR process; as expected, the higher the parameter, the less corrections allowed during the ASR process. This results in a lower percentage of clean portions of $\mathbf{X}_{\text{denoised}}$ (Fig. 3). For a very large value of κ , no more corrections are induced by the ASR process, which leads to leave data unchanged. This converges to a constant percentage of clean data that represents \mathbf{X}_0 ; its value depends on the z-score interval : it is about 60% for [-3.5, 3], 70% for [-3.5, 4] and 80% for [-3.5, 5]. The higher the z-score interval, the more data are considered as clean. In the following, the z-scores values are set to [-3.5, 4].

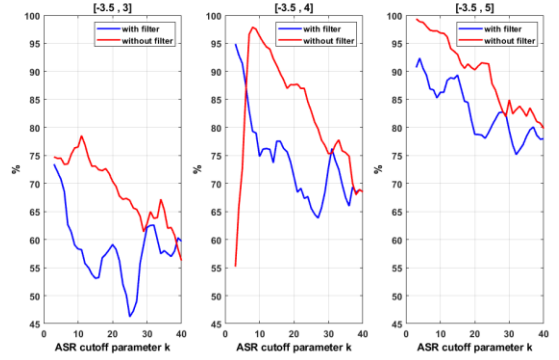


Figure 3. Percentage of clean portions on the denoised data by ASR with different cutoff parameters and different z-scores intervals.

Moreover, we propose to denoise simultaneously both EEG and fNIRS measurements using the ASR method. The signals are z-scored before ASR processing. Three configurations are considered: In the first configuration, the IIR-filter defined in ASR method is applied on both modalities before computing artefact statistics. In the second case, statistics are computed on raw data for both EEG and fNIRS signals. Finally, in the third configuration, the filter is only applied to the EEG signal. These configurations are assessed in terms of percentage of clean portions on the denoised data as previously. Results in Fig.4 show that the best performance is obtained when the IIR-filter is not applied for $\kappa > 6$; for $\kappa = 10$, 88% of clean portions on the denoised data is achieved with the second configuration, while, 70% and 81% are obtained with the first and third configuration respectively. For $\kappa < 6$, the results are almost equivalent between the second and third configurations (raw data and filter on EEG only). Considering these results, we retain the configuration without any filter in the following.

Now this criterion - percentage of clean portions on denoised data $\mathbf{X}_{\text{denoised}}$ is not sufficient to determine the best ASR cutoff parameter to be used. Indeed, a high percentage may induce an excessive cleaning process, co-responsive to non-physiological changes in the initial signals. That is why we propose a second criterion, which computes the percentage of the retained data from the original set. The higher the value of κ , the higher the percentage of retained data and the lower is the percentage of clean portions onto the denoised data (Fig. 5).

The value of κ should then be selected such that brain activities would be preserved and the percentage of clean portions on the denoised data would be high. Here, we opt for the value of $\kappa = 5$. This value seems to be aggressive as only 64% of initial data is retained. However, we should recall that our measurement does not involve any neuro information. It is rather composed of regularly-occurring large amplitude artefacts that are hard to remove without aggressive cutoff parameter [3]. Visual inspection of the data before and after ASR cleaning (Fig.6) shows that the method is efficient in cleaning both EEG and fNIRS signals.

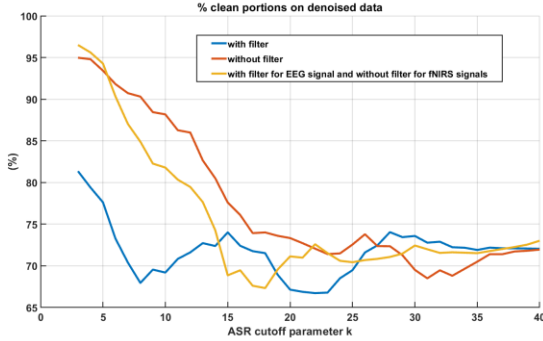


Figure 4. Percentage of clean portions on denoised data with different cutoff parameters and with different configurations.

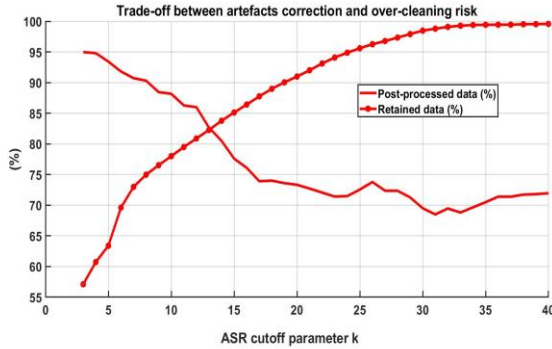


Figure 5. Percentage of post-processed cleaned data and percentage of retained data with different cutoff parameters, without the IIR-filter.

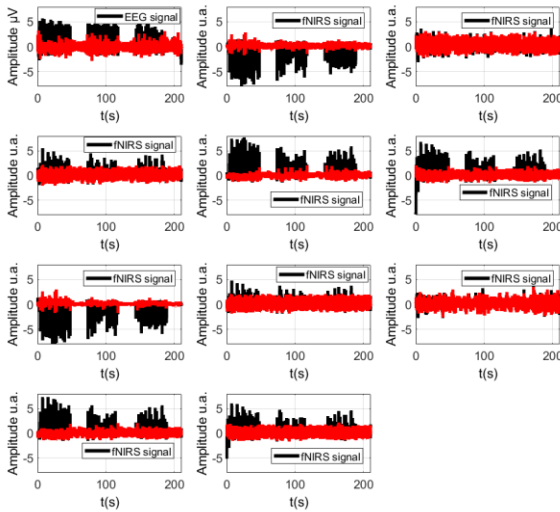


Figure 6. EEG and fNIRS signals without filter before (black curve) and after (red curve) ASR cleaning, $\kappa = 5$.

IV. CONCLUSION

In this paper, we have presented a more comprehensive formulation of ASR that may open different variants. In addition, we have examined the effectiveness of the method in cleaning first fNIRS signals, then fNIRS-EEG measurements from eye-blinking artefacts in the EEG and motion artefacts in the fNIRS. Results showed that the method can be used as one

single, robust and automatic data-cleaning method for both modalities.

The use of one single data-cleaning method may facilitate combining both modalities, taking advantage of them to obtain more accurate results than the individual modalities alone. Moreover, the combination of the two modalities allows the use of the ASR approach even in case of limited number of channels, one modality helping the other in the correction process.

In the near future, the method will be tested on larger data set where artefacts of both modalities are spontaneously generated and the choice of best value of the ASR cutoff parameter may be discussed from the percentage of retained data and that of clean portions on the denoised data.

REFERENCES

- [1] Pierre Comon. Independent Component Analysis. J-L.Lacoume. Higher-Order Statistics, Elsevier, 1992, pp.29-38.
- [2] A. Belouchrani, K. Abed-Meraim, J-F Cardoso, E. Moulines, "A blind source separation technique using second-order statistics", *IEEE Transactions on signal processing*, vol. 45, no. 2, pp. 434-444, Feb. 1997.
- [3] C. -Y. Chang, S. -H. Hsu, L. Pion-Tonachini and T. -P. Jung, "Evaluation of Artifact Subspace Reconstruction for Automatic Artifact Components Removal in Multi-Channel EEG Recordings," *IEEE Transactions on Biomedical Engineering*, vol. 67, no. 4, pp. 1114-1121, April 2020.
- [4] T. R. Mullen et al., "Real-time modeling and 3D visualization of source dynamics and connectivity using wearable EEG," *35th Annual International Conference of the IEEE Engineering in Medicine and Biology Society (EMBC)*, Osaka, Japan, 2013, pp. 2184-2187,
- [5] T. R. Mullen et al., "Real-time neuroimaging and cognitive monitoring using wearable dry EEG," *IEEE Trans. Biomed. Eng.*, vol. 62, no. 11, pp. 2553–2567, Nov. 2015.
- [6] A. Delorme and S. Makeig, "EEGLAB: An open source toolbox for analysis of single-trial EEG dynamics including independent component analysis," *J. Neurosci. Methods*, vol. 134, no. 1, pp. 9–12, 2004 .
- [7] S. Brigadoi, L. Ceccherini, S. Cutini, F. Scarpa, P. Scatturin, J.Selb, L. Gagnon, D. A Boas, R. J Cooper, "Motion artifacts in functional near-infrared spectroscopy: a comparison of motion correction techniques applied to real cognitive data", *NeuroImage*, vol. 85, Part 1, pp. 181-191, 15 January 2014.
- [8] I. Tachtsidis, F. Scholkmann, "False positives and false negatives in functional near-infrared spectroscopy: issues, challenges, and the way forward", *Neurophotonics*, vol. 3, no. 3, pp 031405-1 – 031405-6, 2016
- [9] A. Kessy, A. Lewin, K. Strimmer, "Optimal whitening and decorrelation", *The American Statistician*, vol. 72, no. 4, pp. 309-314, 2018.